

*Neural correlates of stimulus spatial
frequency-dependent contrast detection*

**Jianjun Meng, Ruilong Liu, Ke Wang,
Tianmiao Hua, Zhong-Lin Lu & Minmin
Xi**

Experimental Brain Research

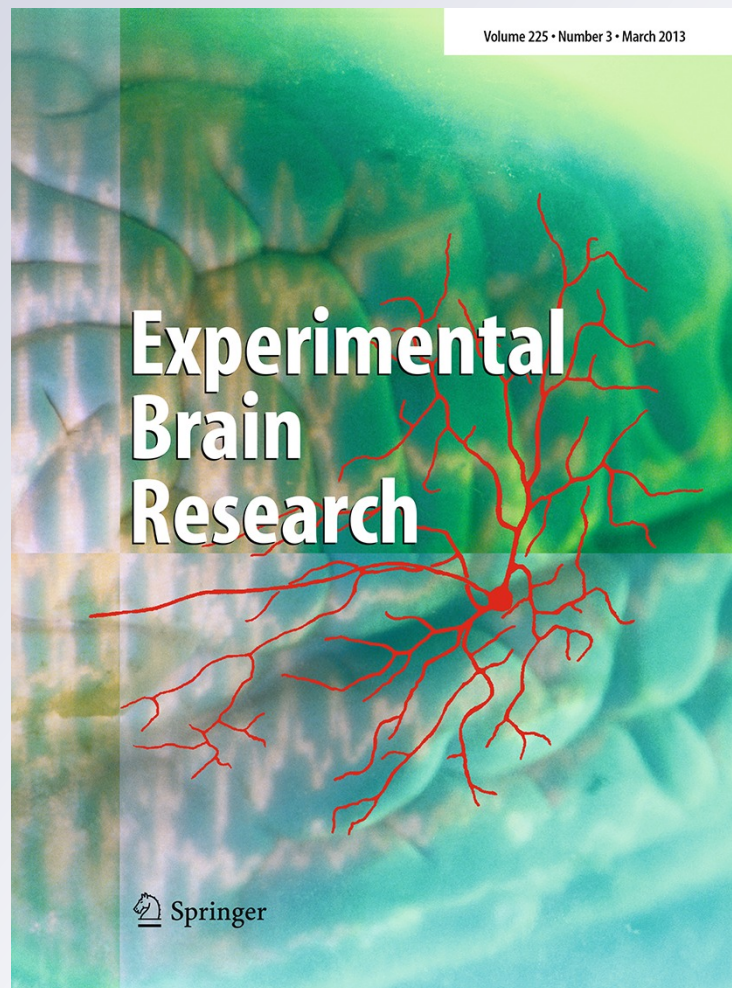
ISSN 0014-4819

Volume 225

Number 3

Exp Brain Res (2013) 225:377-385

DOI 10.1007/s00221-012-3378-z



 Springer

Your article is protected by copyright and all rights are held exclusively by Springer-Verlag Berlin Heidelberg. This e-offprint is for personal use only and shall not be self-archived in electronic repositories. If you wish to self-archive your work, please use the accepted author's version for posting to your own website or your institution's repository. You may further deposit the accepted author's version on a funder's repository at a funder's request, provided it is not made publicly available until 12 months after publication.

Neural correlates of stimulus spatial frequency-dependent contrast detection

Jianjun Meng · Ruilong Liu · Ke Wang ·
Tianmiao Hua · Zhong-Lin Lu · Minmin Xi

Received: 30 March 2012 / Accepted: 8 December 2012 / Published online: 12 January 2013
© Springer-Verlag Berlin Heidelberg 2013

Abstract Psychophysical studies on human and non-human vertebrate species have shown that visual contrast sensitivity function (CSF) peaks at a certain stimulus spatial frequency and declines in both lower and higher spatial frequencies. The underlying neural substrate and mechanisms remain in debate. Here, we investigated the role of primary visual cortex (V1: area 17) in spatial frequency-dependent contrast detection in cats. Perceptual CSFs of three cats were measured using a two-alternative forced-choice task. The responses of V1 neurons to their optimal visual stimuli in a range of luminance contrast levels (from 0 to 1.0) were recorded subsequently using *in vivo* extracellular single-unit recording techniques. The contrast sensitivity of each neuron was determined. The neuronal CSF for each cat was constructed from the mean contrast sensitivity of neurons with different preferred stimulus spatial frequencies. Result: (1) The perceptual and neuronal CSFs of each of the three cats exhibited a similar shape with peak amplitude near 0.4 cpd. (2) The neuronal CSF of each cat was highly correlated with its perceptual CSF. (3) V1 neurons with different preferred stimulus spatial frequencies had different contrast gains. Conclusion: (1) Contrast detection of visual

stimuli with different spatial frequencies may likely involve population coding of V1 neurons with different preferred stimulus spatial frequencies. (2) Difference in contrast gain may underlie the observed contrast sensitivity variation of V1 neurons with different preferred stimulus spatial frequencies, possibly from either evolution or postnatal visual experiences.

Keywords Contrast detection · Spatial frequency · Neural correlates · Visual cortical neurons · Cat

Introduction

Psychophysical investigations on human and vertebrate animals have shown that visual contrast sensitivity depends strongly on stimulus spatial frequency (SF) (Bisti and Maffei 1974; Uhlrich et al. 1981; Hodos et al. 2002; Sowden et al. 2002; Jarvis and Wathes 2008). Across species, the CSFs have a similar inverted-U shape with a single peak, although the spatial frequency domain varies in different species and the peak of the CSF shifts slightly with stimulus size and luminance (Uhlrich et al. 1981; Jarvis and Wathes 2008). Despite a progressive understanding that detection or discrimination of visual stimuli is related to the contrast–response functions of visual cortical neurons, the mechanism underlying the CSF has not been fully understood (Virsu and Rovamo 1979; Barlow et al. 1987; Geisler and Albrecht 1997; Boynton et al. 1999; Goris et al. 2009).

Based on the modulation transfer function (MTF) theory, Rovamo and Barton developed a model that related three important pre-cortical processes to perceptual CSF (Rovamo et al. 1993; Barten 1999). Although this model can predict the overall SF domain and the inverted-U shape of CSFs for human and non-human species, it treats the cortical detection

J. Meng · R. Liu · K. Wang · T. Hua (✉)
College of Life Sciences, Anhui Normal University,
Wuhu 241000, China
e-mail: tmhua@mail.ahnu.edu.cn

Z.-L. Lu (✉)
Laboratory of Brain Processes (LOBES), Department
of Psychology, The Ohio State University, Columbus,
OH 43210, USA
e-mail: lu.535@osu.edu

M. Xi
Management School, Queen's University, 25 University Square,
Belfast BT7 1NN, UK

process as a scaling constant and ignores its contribution to the overall magnitude differences in perceptual CSFs between species (Jarvis and Wathes 2008). On the other hand, some authors found that CSFs constructed from visual evoked potentials were similar to perceptual CSF in terms of the overall shape, peak location, and SF domain (Berkley and Watkins 1973; Campbell et al. 1973). These observations suggest that visual contrast sensitivities at different SFs are closely related to neuronal activities in the visual cortex. Further, Boynton and colleagues compared human psychophysical contrast increment thresholds with neuronal activities inferred from BOLD fMRI signals. They found that the contrast gain in early visual cortical areas depends systematically on stimulus SF and concluded that contrast discrimination judgements are limited by pooled activities of neurons in early visual cortical areas (Boynton et al. 1999). There is, however, no direct electrophysiological evidence to support these points of view, and it remains unknown whether CSFs constructed from neuronal responses in early visual cortical areas can predict perceptual CSFs.

In this study, we intend to examine whether the perceptual CSF can be predicted from the CSF derived from neuronal responses in V1. To this end, we measured the perceptual CSFs for three cats after conditioning training, which was followed by single-unit recording of neuronal responses of cells in V1 to their respective optimal stimulus in a range of luminance contrasts (0–1.0). The contrast sensitivity of each neuron was assessed from its contrast–response function. The neuronal CSF of each cat was constructed from the mean contrast sensitivity of V1 neurons with different preferred stimulus spatial frequencies and was then compared with the corresponding perceptual CSF. Additionally, we compared the properties of the contrast–response functions of neurons with different preferred spatial frequencies, in an attempt to understand the mechanism underlying spatial frequency-dependent neuronal contrast sensitivity.

Experimental procedure

Subjects

Three adult male cats (age: 2–2.5 years old; body weight: 2–2.4 kg) with no optical or retinal problems served as subjects. All cats were housed in one room and maintained on a 12 h: 12 h light/dark cycle (lights on at 7 am) with ad libitum water available. All cats received training in a grating orientation identification task and could get enough food reward during the 2–3-h training period on each weekday and were given free access to food on the weekends. Animal treatments were strictly in accordance with the National Institutes of Health Guide for the Care and Use of Laboratory Animals.

Psychophysical procedures

The training apparatus was similar to that described in previous publications (Blake and Petrakis 1984; Orban et al. 1990; Hua et al. 2010). All cats performed a two-alternative forced-choice grating orientation identification task presented on a CRT and acquired food reward by pushing the correct (left or right) nose key in every trial. The visual stimuli were windowed sinusoidal gratings generated by MATLAB programs based on Psychtoolbox (Brainard 1997) and presented in the center of the CRT. The circular window was 16 cm or 8° visual angle in diameter at a 57-cm viewing distance.

At first, cats received conditioning training in a two-alternative forced-choice grating detection task with fixed, high-contrast (80 %) grating stimuli at a single spatial frequency, which were oriented $\pm 45^\circ$. To ensure that the measured perceptual CSFs were not biased by the spatial frequency of the conditioning stimulus, we used 0.2 cpd for Cat1, 0.4 cpd for Cat2, and 0.6 cpd for Cat3 during conditioning (Fig. 1a–c). The mean luminance of the grating stimuli was 19 cd/m², and the environmental ambient luminance on the cornea was 0.1 lux. In each daily training session, the subject was administered 800–1,200 trials in 10–15 80-trial blocks. Subjects took a 5-min break between blocks. The experimenter triggered the first trial in the beginning of each training block when everything was ready. Each trial started with a flashing (3 Hz) bright fixation dot (0.1° visual angle) that appeared in the center of the CRT for 1 s. This was followed by a 4-s stimulus presentation with a 1-s response denied period (RDP) during which pushing the nose keys triggered no food reward. Because large-size sine-wave gratings were used in the study, eye fixation was not important and not monitored. A four-second inter-trial interval (ITI) was provided between trials.

All cats concluded their conditioning training after ≥ 90 % correct performance was attained in 6 consecutive days. This was then followed by measurements of the psychophysical contrast sensitivity function. Contrast thresholds at 0.1, 0.2, 0.4, 0.6, 0.8, 1.2, and 1.6 cpd (800 trials of test for each SF; all intermixed) were measured to construct ten repeated measures of the CSF, one from every 80 trials at each spatial frequency.

A 2-correct down/1-error up staircase procedure was used to measure contrast thresholds: Stimulus contrast in each trial was reduced to 0.9 times of that of the previous trial if the subject made correct responses in two consecutive trials or increased to 1.1 times if the subject made an incorrect response in the previous trial. The procedure asymptotically converges to a contrast threshold at 70.7 % correct. A reversal results when the staircase changes from increasing to decreasing contrast or vice versa. Following standard practice, we averaged the contrasts of an even number of

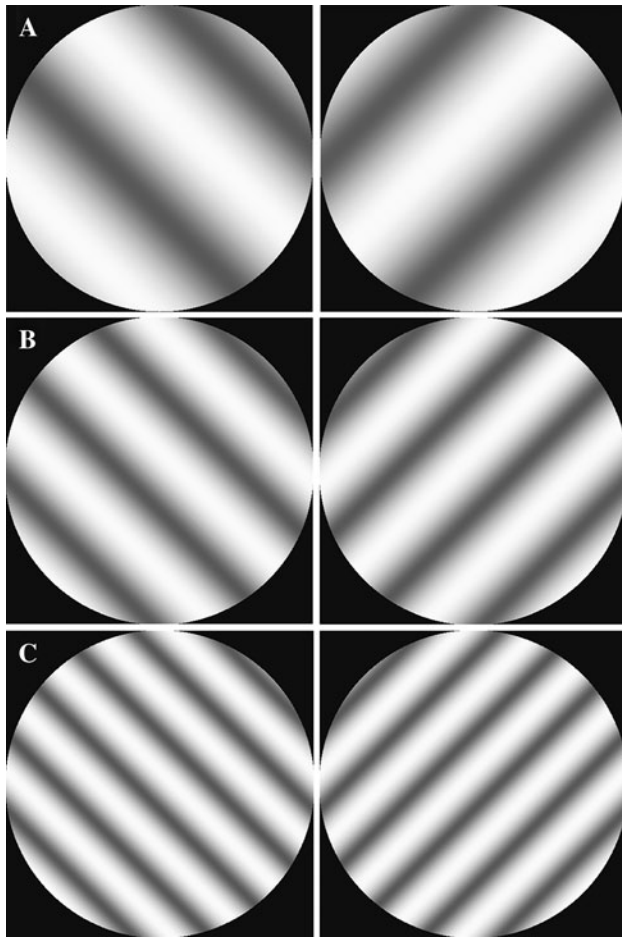


Fig. 1 Visual signals A, B, and C were used for conditioning training of cat1, cat2, and cat3. For all three cats, stimuli were sine-wave gratings oriented $\pm 45^\circ$. All gratings had a fixed mean luminance of 19 cd/m^2 and contrast of 80 %. The spatial frequency of the gratings was set at 0.2, 0.4, and 0.6 cpd for cat1, cat2, and cat3, respectively

reversals to estimate the contrast threshold. Contrast sensitivity at each spatial frequency was defined as the log of the reciprocal of the mean threshold contrast value. The contrast sensitivity functions were fit with the Gaussian equation:

$$\text{CSF}(f) = \text{CSF}_0 + A \exp \left[-\frac{(f-f_0)^2}{\text{width}^2} \right], \quad (1)$$

where f is the spatial frequency of the grating, A is the maximum sensitivity, f_0 is the peak spatial frequency, and width is related to the low and high cutoff spatial frequencies of the CSF.

Electrophysiological recording

Following the psychophysical measurement of CSF, all three cats were prepared for extracellular single-unit recording using procedures described in previous publications (Hua et al. 2006, 2009). Briefly, cats were anesthetized with

ketamine HCl (40 mg/kg) and xylazine (2 mg/kg). After the intravenous and tracheal cannulae were inserted, cats were placed in a stereotaxic apparatus. Pupils were maximally dilated with atropine (1 %) and fitted with contact lens (no power) to protect the cornea from dryness. An artificial pupil (4 mm in diameter) was placed in front of the cornea, as close to the contact lens as possible. Neosynephrine (5 %) was administered to retract the nictitating membranes. A mixture of urethane (20 mg/h/kg body weight) and gallamine triethiodide (10 mg/h/kg body weight) was infused intravenously to maintain anesthesia and paralysis. Expired pCO_2 was maintained at approximately 3.8 %. Heart rate (about 180–220 pulses/min) and EKG were monitored throughout the experiment to assess the level of anesthesia and ensure that the animals were not responding to pain. A small hole was drilled in the skull 4 mm posterior to the ear bars and 2 mm lateral to the midline. A glass-coated tungsten microelectrode (with an impedance of 3–5 M Ω) was positioned and advanced using a hydraulic micromanipulator (NARISHIGE, Japan). The small hole was filled with a 4 % agar solution in saline and sealed with wax. Prior to each penetration, we removed the agar over the cortex and dried the cortical surface with soft tissue, and then covered the cortex again with agar after the microelectrode made contact with the cortical surface. To ensure that we randomly sampled neurons from all cortical layers, we confined electrode penetrations (at least 20 penetrations for each cat, with $\geq 400 \mu\text{m}$ inter-penetrations space) in the medial bank of the lateral gyrus (V1), a region where the cortical surface ran approximately parallel to the white matter (Hua et al. 2008), and isolated units at a vertical depth within $2,000 \mu\text{m}$ from the pial surface at each penetration.

After completing all pre-recording preparations, the optic disks of the two eyes were reflected onto a movable transparent tangent screen, which overlapped with the CRT monitor used for stimulus presentation. The area centralis of each eye was located prior to physiological recording based on the position of the optic disks reflected onto the tangent screen (Bishop et al. 1962).

Single-unit responses were measured with moving sinusoidal gratings generated with MATLAB programs based on Psychophysics Toolbox (Brainard 1997). The mean luminance of the grating stimuli and the environmental ambient luminance on the cornea were the same as those used in psychophysical experiments. The visual stimuli were shown on the CRT monitor (resolution $1,024 \times 768$, refresh rate 85 Hz), placed 57 cm away from the animal's eyes. When a single unit was isolated, the center of the cell's receptive field was carefully mapped by consecutively presenting a series of computer-generated light spots on the CRT and then marked on the movable transparent tangent screen. Next, we determined the optimal grating stimulus (optimal orientation and motion direction, spatial and temporal frequency,

and size) for each cell by presenting a series of stimulus conditions. Correct focus of artificial pupil was established by comparing the cell's responses to gratings with different spatial frequencies as different spectacle lens were in place. Subsequently, neuronal responses to the optimal stimuli with varied contrast levels (0–1: 0, 0.01, 0.04, 0.09, 0.16, 0.25, 0.36, 0.49, 0.64, 0.81, and 1.0) were systematically recorded. The sequence of stimulus presentations at different contrast levels was randomized with each stimulus presented 4–6 times to the dominant eye. The duration of each stimulus presentation was less than 5 s (varied with temporal frequency of the stimulus). There was a 2-min interval between stimulus repeats for functional recovery of the recorded neuron. Single-unit recordings were made in the central visual field of both eyes. After recording, the eccentricity of the receptive field of each cell was determined by measuring the distance between the center of the receptive field and the area centralis of the animal's dominant eye.

After the signal was amplified with a microelectrode amplifier (NIHON KOHDEN, Japan) and differential amplifier (Dagan 2400A, USA), action potentials were fed into a window discriminator with an audio monitor. The original voltage traces were digitized using an acquisition board (National Instruments, USA) controlled by IGOR (WaveMetrics, USA) and saved for later analysis. Post-stimulus time histograms (PSTHs) of the response were also obtained. The response of a cell to a drifting sinusoidal grating was defined as the mean response value corresponding to the time of stimulus modulation, which was used to draw the response-contrast tuning curve (Fig. 2a, b). The preferred stimulus orientation, motion direction, spatial and temporal frequency, and size for each cell were pre-determined as previously described (Schmolesky et al. 2000; Hua et al. 2006). Because a previous study showed that V1 neurons generally sharpened their response tuning

curves around the preferred stimulus spatial frequency as stimulus contrast decreased toward a threshold level (Sceniak et al. 2002), we chose the contrast sensitivity at the preferred stimulus spatial frequency as the best measurement of each neuron's contrast sensitivity. Based on recent studies that suggest that the visual system may combine information across neurons tuned to different spatial frequencies in processing low-contrast sinusoidal gratings (Goris et al. 2009; Hua et al. 2010), we constructed neuronal CSFs from the mean contrast sensitivity of V1 neurons with different preferred stimulus spatial frequencies. To determine the contrast sensitivity of each V1 neuron, we fitted its contrast–response function with the Naka-Rushton equation (Albrecht 1995) (Fig. 2b):

$$R(C) = R_{\max} \frac{C^N}{C^N + C_{50}^N} + M, \tag{2}$$

in which $R(C)$ represents the neuron's visually driven response to a visual stimulus with contrast value of C , R_{\max} is the neuron's maximal visually evoked response to visual stimuli, M is the neuron's spontaneous activity or baseline response, C_{50} corresponds to the stimulus contrast that evokes half of the neuron's maximal response, and N represents the slope of the neuron's response-contrast function. Threshold contrast (T_c) of each neuron is defined as the contrast that evokes a response that is 1.414 times of its baseline response (M) (Hua et al. 2010). Contrast sensitivity of a neuron was represented by the inverse of its T_c , called T_c -contrast sensitivity (TcCS). Cells with less than 95 % goodness of fit were not included in our data analysis.

Statistical comparisons between cell populations responding preferentially to different SFs were carried out using ANOVA. All values were expressed as mean \pm standard deviation (SD) or standard error of the mean (SEM).

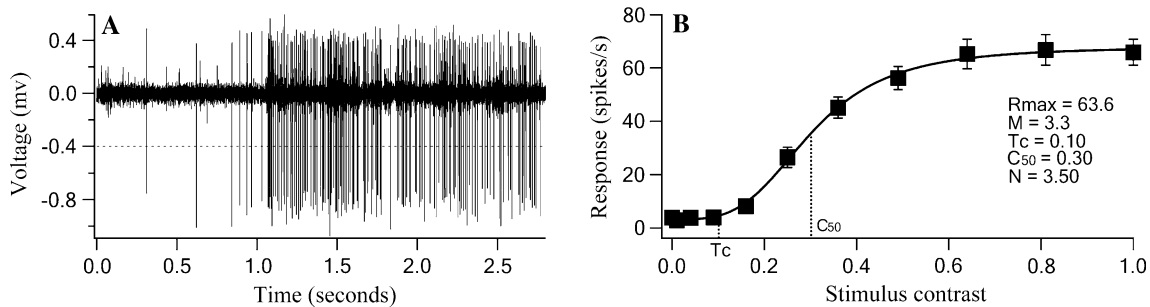


Fig. 2 A typical neuron's response to its optimal visual stimulus. **a** The voltage trace of the neuron's response to the optimal stimulus at 64 % contrast. A spike with an amplitude surpassing the horizontal broken line is counted as an action potential. The neuron's response was evoked by 5 cycles of grating stimulation, equivalent to a stimulus duration of about 1.7 s. Spontaneous activity (M) was acquired 1 s prior to visual stimulus presentation. **b** Contrast–response function of

the neuron (mean \pm SD). The smooth curve represents the best fitting Naka-Rushton equation ($r^2 = 99.2\%$). M and R_{\max} represent the neuron's spontaneous activity and maximal visually evoked response to visual stimuli. C_{50} denotes the stimulus contrast that evokes half of the neuron's maximal response. N represents the slope of the neuron's contrast–response curve. T_c is the threshold stimulus contrast that evokes a response 1.414 times of the neuron's spontaneous activity

Results

Perceptual contrast sensitivity function

All three cats (cat1, cat2, and cat3) succeeded in conditioning training, that is, identifying the orientation ($\pm 45^\circ$) of high contrast (80 %) sinusoidal gratings at $>90\%$ correct performance for six consecutive days after 3–5 months of training.

ANOVA indicated that the contrast sensitivity function (CSF) of each cat showed a significant main effect of stimulus spatial frequency (SF) (Cat1: $F(6,63) = 63.47$, Cat2: $F(6,63) = 169.2$, Cat3: $F(6,63) = 92.99$, all $p < 0.0001$). Based on the best fitting Gaussian function (Eq. 1), the CSFs peaked around 0.4 cpd for all three cats (Cat1: 0.37 cpd; Cat2: 0.37 cpd; Cat3: 0.39 cpd) (Fig. 3a–c). The CSFs were

significantly different among the cats ($F(2,189) = 9.725$, $p < 0.001$), but exhibited no significant SF/cat interaction ($F(12,189) = 1.686$, $p > 0.10$). This result suggests that the three cats showed a varied ability in visual contrast detection at different SFs, but their CSFs shared a similar shape.

Neuronal contrast sensitivity functions

To uncover the neural correlates of perceptual contrast sensitivity function, we calculated the mean contrast sensitivity of V1 neurons with different preferred stimulus spatial frequencies using the reciprocal of their threshold contrasts (T_c). A total of 66 cells from Cat1, 69 cells from Cat2, and 68 cells from Cat3 were studied (Table 1). The receptive fields of all cells included in this study were located within 8° of the central area of the dominant eye.

ANOVA indicated that the neuronal CSF (T_c -contrast sensitivity function) in each cat exhibited a significant main effect of stimulus spatial frequency (Cat1: $F(6,59) = 5.258$; Cat2: $F(6,62) = 21.83$; Cat3: $F(6,61) = 9.586$, all $p < 0.0001$). Based on the best fitting Gaussian function Eq. (1), the neuronal CSFs also reached their peaks around 0.4 cpd (Cat1: 0.39 cpd; Cat2: 0.38 cpd; Cat3: 0.38 cpd) (Fig. 3a–c). The neuronal CSFs showed significant differences between cats ($F(2,182) = 3.784$, $p < 0.05$), but no SF/cat interaction ($F(12,182) = 0.333$, $p > 0.5$).

Comparison between perceptual and neuronal CSFs

To examine the relationship between neuronal and perceptual CSFs, we computed the correlation between them for each cat.

The neuronal CSF in each cat was highly correlated with the corresponding perceptual CSF (Cat1: $R = 0.990$, $p < 0.0001$; Cat2: $R = 0.996$, $p < 0.0001$; Cat3: $R = 0.991$, $p < 0.0001$). As shown in Fig. 4, linear regression of neuronal versus perceptual CSFs was excellent for all three cats (all $p < 0.0001$). This result suggests that perceptual contrast sensitivities at different SFs are linearly correlated with the mean contrast sensitivities of V1 neurons responding preferentially to stimuli with the corresponding SFs.

Mechanisms of contrast sensitivity of V1 neurons

Contrast sensitivity variation of V1 neurons with different preferred stimulus SFs may depend on four factors (Li et al. 2008; Hua et al. 2010): (1) Spontaneous activity (M), (2) Maximal response (R_{max}), (3) Slope of the contrast–response function (N), and (4) Contrast gain ($1/C_{50}$). To test these possibilities, we systematically compared the best fitting parameters of the Naka-Rushton equation between neurons with different preferred spatial frequencies.

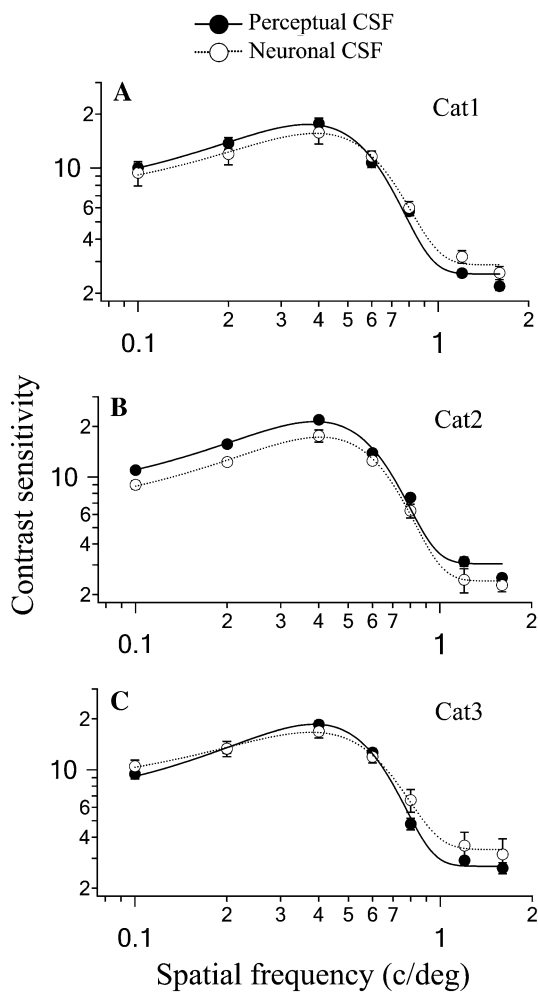


Fig. 3 Perceptual and neuronal CSFs (contrast sensitivity functions) of three cats. The filled and open circles with error bars (1 SEM) represent the perceptual and neuronal contrast sensitivity at different SFs, respectively. The solid and dotted lines are the best fits to the perceptual and neuronal CSFs, respectively

Table 1 Mean contrast sensitivity of V1 neurons with different preferred stimulus spatial frequencies

Subjects	N/CS	Spatial frequency (cpd)						
		0.1	0.2	0.4	0.6	0.8	1.2	1.6
Cat1	N	10	20	15	7	5	5	4
	TcCS	9.3 ± 1.5	11.2 ± 1.6	15.8 ± 2.2	11.6 ± 0.8	5.9 ± 0.5	3.3 ± 0.3	2.6 ± 0.2
Cat2	N	10	16	20	11	5	4	3
	TcCS	9.0 ± 0.5	12.3 ± 0.5	17.6 ± 1.5	12.5 ± 0.4	6.3 ± 0.6	2.5 ± 0.4	2.2 ± 0.2
Cat3	N	6	10	22	14	9	4	3
	TcCS	10.5 ± 0.9	13.3 ± 1.4	16.9 ± 1.4	11.9 ± 0.9	6.6 ± 1.0	3.6 ± 0.7	3.2 ± 0.7

N and CS represent cells number and contrast sensitivity, respectively. TcCS is T_c -contrast sensitivity ($1/T_c$), which is expressed as Mean ± 1SEM

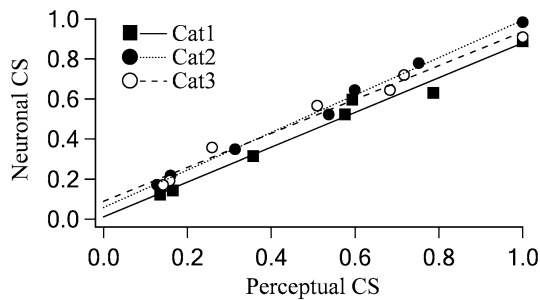


Fig. 4 Scatter plots of neuronal versus perceptual CS at different SFs (0.1, 0.2, 0.4, 0.6, 0.8, 1.2, and 1.6 cpd) for each of the three cats (Filled square Cat1; Filled circle Cat2; Open circle Cat3). The neuronal and perceptual CS values were normalized to their maximum for each cat. The solid, dotted, and broken lines are the best linear regressions

No significant variation was found between neurons responding preferentially to stimuli with different SFs in terms of spontaneous activity ($F(6,182) = 0.228, p > 0.5$), maximal response ($F(6,182) = 0.373, p > 0.5$), and slope of the contrast–response function ($F(6,182) = 0.318, p > 0.5$) (Fig. 5a–c). However, there was a significant difference between neurons with different preferred stimulus spatial frequencies in terms of C_{50} ($F(6,182) = 33.194, p < 0.0001$) (Fig. 5d), and the difference was independent of the subject (interaction of spatial frequency and cat: $F(12,182) = 0.229, p > 0.5$). In each cat, the mean C_{50} value was lowest for neurons with preferred SF at 0.4 cpd, but increased gradually for neurons with preferred SFs higher or lower than 0.4 cpd (Fig. 5d).

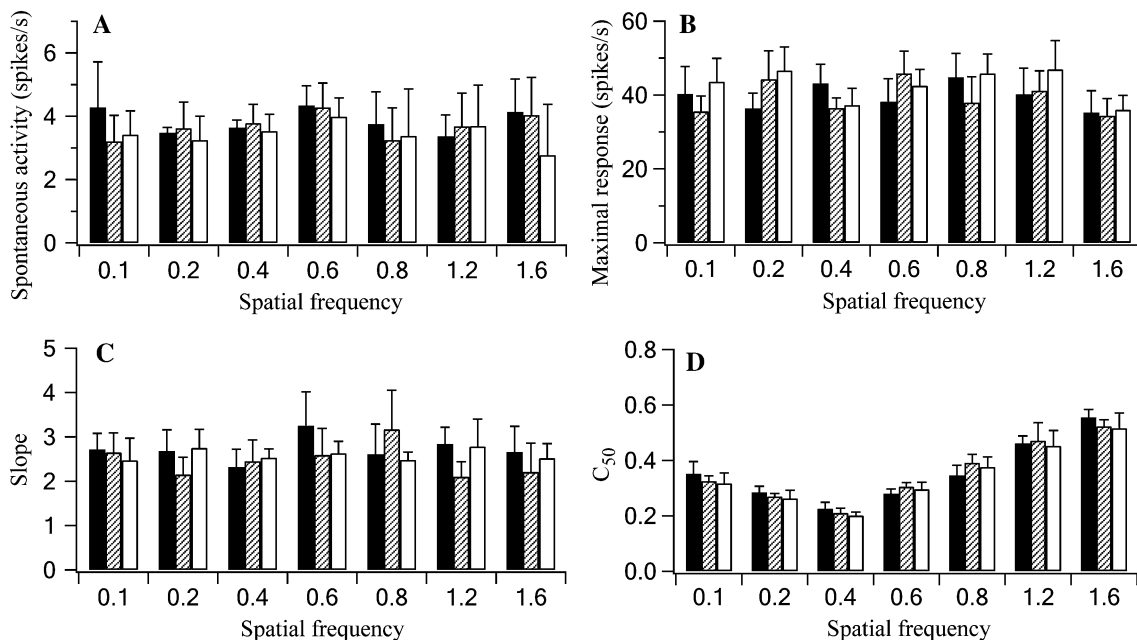


Fig. 5 Spontaneous activity (a), maximal response (b), contrast–response function slope (c), and C_{50} (d) of V1 neurons responding preferentially to different stimulus spatial frequencies. Black, patternrd, and white bars represent Cat1, Cat2, and Cat3, respectively

We conclude that contrast sensitivity changes of V1 neurons with different preferred stimulus spatial frequencies may result from different contrast gains. Neurons with preferred SFs closer to the optimal perceptual SF (0.4 cpd) have higher contrast gains (lower C_{50}), whereas neurons with preferred SFs away from the optimal perceptual SF have lower contrast gains (higher C_{50}).

Discussion

Perceptual CSFs

In this study, perceptual CSFs of three cats were measured using a 2-AFC task with a 2-down/1-up staircase procedure. The CSFs of the three cats shared similar shapes and peak spatial frequencies, although there were some differences.

The overall amplitude of the perceptual CSFs in our study is significantly lower than that in previous studies (Blake et al. 1974; Pasternak and Merigan 1981). Pasternak and Merigan used a stimulus luminance (16 cd/m²) quite close to ours and a size (11°–14° visual angle) slightly larger than ours but reported a CSF amplitude higher than ours (Pasternak and Merigan 1981). Therefore, the CSF amplitude difference could not be attributed to variations of stimulus luminance and size. It is likely that other factors may contribute to the difference: (1) The task in our study, identification of a $\pm 45^\circ$ grating near threshold, is different from detecting a grating on a uniform background used in the literature; (2) In this study, the CSFs were constructed based on an average of 10 blocks (80 trials/block) of contrast threshold measurements at each SF. On each testing day, tests at different SFs were pseudorandomly interleaved. Previous studies measured CSFs by continuously tracking contrast threshold at each SF till asymptotic performance, which could have over-estimated the contrast sensitivity at each SF.

Neural basis of contrast detection or discrimination

The neural basis mediating contrast detection or discrimination has been investigated for more than 30 years. Some authors recorded from single neurons in cat and monkey primary visual cortex and compared the contrast–response functions of V1 neurons with behavioral measures of absolute contrast detection thresholds (Tolhurst et al. 1983; Hawken and Parker 1990). They found that behavioral thresholds could be well predicted by the responses of the most sensitive single neurons. Geisler and Albrecht recorded the responses of neurons from the primary visual cortex of cats and monkeys and used those measurements to predict entire contrast discrimination threshold curves. They showed that behavioral contrast discrimination functions were similar in shape to the neuronal discrimination

functions of the most sensitive cells and the contrast discrimination functions obtained by optimal pooling of the entire population of cells (Geisler and Albrecht 1997; Clatworthy et al. 2003; Chirimuuta and Tolhurst 2005).

Why behavioral contrast detection or discrimination sensitivity varies with stimulus spatial frequency has also been explored by some researchers. A theoretical model proposed by Rovamo and Barton (Barten 1999; Rovamo et al. 1999; Jarvis and Wathes 2007, 2008) suggests that three important pre-cortical factors, including image formation through the optics of the eye, and receptor sampling and lateral inhibition in the retina, contribute to spatial vision characterized by contrast sensitivity. Recent investigations showed that the Rovamo–Barton model could describe the overall spatial contrast sensitivity in a diverse range of species (Jarvis and Wathes 2007, 2008; Jarvis et al. 2009). However, this model ignored the role of visual cortex and treated cortical processing as a scaling constant (Jarvis and Wathes 2008). Other studies indicated that neurons in visual cortex, rather than subcortical locations, played a major part in contrast gain control (Ohzawa et al. 1985; McLean and Palmer 1996; Sanchez-Vives et al. 2000). In this research, we first measured the perceptual CSF in three cats and then constructed neuronal CSF based on the contrast–response functions of V1 neurons with different preferred stimulus spatial frequencies. We found that the neuronal and perceptual CSFs in each cat were highly correlated; they shared a very similar shape, peak SF, and amplitude in the measured range of SFs. These results suggest that the neural site responsible for SF-dependent contrast detection might be in V1. This conclusion is consistent with a previous fMRI study, which demonstrates that neuronal signals that are correlated with performance in contrast discrimination are presented in V1 (Boynton et al. 1999).

Mechanism of contrast sensitivity variation of V1 neurons

As shown in this study, V1 neurons with different preferred stimulus SFs exhibited different contrast sensitivities. This could result from changes of spontaneous activity (M), maximal response (R_{\max}), slope of contrast–response function (N), and/or contrast gain ($1/C_{50}$) (Li et al. 2008; Lu and Doshier 2008). Through systematic comparison, we found that the variation of contrast sensitivity of V1 neurons with different preferred stimulus SFs did not result from changes of spontaneous activity, nor maximal response, nor slope of the contrast–response functions (Fig. 5a–c), but rather from differential contrast gains. Neurons with preferred SFs near the optimal perceptual SF (0.4 cpd) had higher contrast gains, whereas neurons with preferred SFs higher or lower than the optimal perceptual SF had lower contrast gains. This result indicates that contrast sensitivity differences of V1 neurons with different preferred stimulus SFs might be

caused by contrast-gain variations in different neuronal populations, which could be an important cellular mechanism underlying SF-dependent contrast detection. Our result was consistent with a phenomenon observed in a previous physiological and anatomical study, which reported that striate cortical neurons with different contrast sensitivities displayed to some extent a match for neurons with different optimal SFs according to their distance from the center of cytochrome oxidase (CO) blobs (Edwards et al. 1995).

Why V1 neurons with different preferred SFs show different contrast gains is unclear. Based on the receptive field (RF) architecture of V1 neurons and synaptic transmission theory, we propose that contrast gains of V1 neurons to their preferred stimuli may depend on the density of excitatory synapses or postsynaptic receptors. It is possible that neurons with preferred SFs closer to the optimal perceptual SF have denser synaptic connections with presynaptic excitatory cells or have more postsynaptic receptors, and thus could be easily activated by lower stimulus contrast. Another possibility is that neurons with bigger RFs or lower preferred SFs receive more excitatory synaptic inputs from large-scale horizontal connections, but the integration efficiency of postsynaptic potentials decreases with the distance from the RF center. And neurons with preferred SFs closer to the optimal perceptual SF may achieve larger input-integration ratio and thus exhibit higher contrast gains. Further studies are needed to clarify these possibilities.

Biological significance of contrast sensitivity functions

The observation that visual contrast sensitivity varies with stimulus spatial frequency is a phenomenon common to human and many vertebrate animal species examined (Uhlrich et al. 1981; Sowden et al. 2002; Jarvis and Wathes 2008). Each species is characterized by a certain SF domain within which visual targets are discriminable. Moreover, each species retains an optimal SF at which visual signals are most easily detected even under low luminance contrasts. Such a species-specific property of vision certainly has great implications for animals' daily functions, such as preying and escaping (Northmore and Dvorak 1979). It is unknown how each species develops a characteristic SF domain and optimal SF. One possibility is that different species may retain different genes that based on the visual properties that are most beneficial to its living and social activities. Another possibility is that each species may develop the neural circuits that best match the meaningful visual stimuli presented in its living environment during postnatal visual experiences. In fact, even learning in the adulthood could produce substantial neural plasticity and modify the sensitivity of contrast detection on visual signals (Zhou et al. 2006; Hua et al. 2010). Further studies are needed to clarify these issues.

Acknowledgments This research was supported by the National Natural Science Foundation of China (No. 31171082), US National Eye Institute grants (R01 EY017491 and R01 EY021553), the Natural Science Foundation of Anhui Province (070413138), and the Key Research Foundation of Anhui Province Education Department (KJ2009A167).

References

- Albrecht DG (1995) Visual cortex neurons in monkey and cat: effect of contrast on the spatial and temporal phase transfer functions. *Vis Neurosci* 12:1191–1210
- Barlow HB, Kaushal TP, Hawken M, Parker AJ (1987) Human contrast discrimination and the threshold of cortical neurons. *J Opt Soc Am A*: 4:2366–2371
- Barten PJG (1999) Contrast sensitivity of the human eye and its effects on image quality. SPIE Optical Engineering Press, Washington
- Berkley MA, Watkins DW (1973) Grating resolution and refraction in the cat estimated from evoked cerebral potentials. *Vision Res* 13:403–415
- Bishop PO, Kozak W, Vakkur GJ (1962) Some quantitative aspects of the cat's eye: axis and plane of reference, visual field co-ordinates and optics. *J Physiol* 163:466–502
- Bisti S, Maffei L (1974) Behavioural contrast sensitivity of the cat in various visual meridians. *J Physiol* 241:201–210
- Blake R, Petrakis I (1984) Contrast discrimination in the cat. *Behav Brain Res* 12:155–162
- Blake R, Cool SJ, Crawford ML (1974) Visual resolution in the cat. *Vision Res* 14:1211–1217
- Boynton GM, Demb JB, Glover GH, Heeger DJ (1999) Neuronal basis of contrast discrimination. *Vision Res* 39:257–269
- Brainard DH (1997) The psychophysics toolbox. *Spat Vis* 10:433–436
- Campbell FW, Maffei L, Piccolino M (1973) The contrast sensitivity of the cat. *J Physiol* 229:719–731
- Chirimuuta M, Tolhurst DJ (2005) Does a Bayesian model of V1 contrast coding offer a neurophysiological account of human contrast discrimination? *Vision Res* 45:2943–2959
- Clatworthy PL, Chirimuuta M, Lauritzen JS, Tolhurst DJ (2003) Coding of the contrasts in natural images by populations of neurons in primary visual cortex (V1). *Vision Res* 43:1983–2001
- Edwards DP, Purpura KP, Kaplan E (1995) Contrast sensitivity and spatial frequency response of primate cortical neurons in and around the cytochrome oxidase blobs. *Vision Res* 35:1501–1523
- Geisler WS, Albrecht DG (1997) Visual cortex neurons in monkeys and cats: detection, discrimination, and identification. *Vis Neurosci* 14:897–919
- Goris RL, Wichmann FA, Henning GB (2009) A neurophysiologically plausible population code model for human contrast discrimination. *J Vis* 9:15
- Hawken MJ, Parker AJ (1990) Detection and discrimination mechanisms in the striate cortex of the old-world monkey. In: Blakemore C (ed) *Vision: coding and efficiency*. Cambridge University Press, Cambridge, pp 103–116
- Hodos W, Ghim MM, Potocki A, Fields JN, Storm T (2002) Contrast sensitivity in pigeons: a comparison of behavioral and pattern ERG methods. *Doc Ophthalmol* 104:107–118
- Hua T, Li X, He L, Zhou Y, Wang Y, Leventhal AG (2006) Functional degradation of visual cortical cells in old cats. *Neurobiol Aging* 27:155–162
- Hua T, Kao C, Sun Q, Li X, Zhou Y (2008) Decreased proportion of GABA neurons accompanies age-related degradation of neuronal function in cat striate cortex. *Brain Res Bull* 75:119–125
- Hua T, Li G, Tang C, Wang Z, Chang S (2009) Enhanced adaptation of visual cortical cells to visual stimulation in aged cats. *Neurosci Lett* 451:25–28

- Hua T, Bao P, Huang CB, Wang Z, Xu J, Zhou Y, Lu ZL (2010) Perceptual learning improves contrast sensitivity of V1 neurons in cats. *Curr Biol* 20:887–894
- Jarvis JR, Wathes CM (2007) On the calculation of optical performance factors from vertebrate spatial contrast sensitivity. *Vision Res* 47:2259–2271
- Jarvis JR, Wathes CM (2008) A mechanistic inter-species comparison of spatial contrast sensitivity. *Vision Res* 48:2284–2292
- Jarvis JR, Abeyesinghe SM, McMahon CE, Wathes CM (2009) Measuring and modelling the spatial contrast sensitivity of the chicken (*Gallus g. domesticus*). *Vision Res* 49:1448–1454
- Li X, Lu ZL, Tjan BS, Doshier BA, Chu W (2008) Blood oxygenation level-dependent contrast response functions identify mechanisms of covert attention in early visual areas. *Proc Natl Acad Sci USA* 105:6202–6207
- Lu ZL, Doshier BA (2008) Characterizing observers using external noise and observer models: assessing internal representations with external noise. *Psychol Rev* 115:44–82
- McLean J, Palmer LA (1996) Contrast adaptation and excitatory amino acid receptors in cat striate cortex. *Vis Neurosci* 13:1069–1087
- Northmore DPM, Dvorak CA (1979) Contrast sensitivity and acuity of the goldfish. *Vision Res* 19:255–261
- Ohzawa I, Sclar G, Freeman RD (1985) Contrast gain control in the cat's visual system. *J Neurophysiol* 54:651–667
- Orban GA, Vandenbussche E, Sprague JM, De Weerd P (1990) Orientation discrimination in the cat: a distributed function. *Proc Natl Acad Sci USA* 87:1134–1138
- Pasternak T, Merigan WH (1981) The luminance dependence of spatial vision in the cat. *Vision Res* 21:1333–1339
- Rovamo J, Luntinen O, Nasanen R (1993) Modelling the dependence of contrast sensitivity on grating area and spatial frequency. *Vision Res* 33:2773–2788
- Rovamo JM, Kankaanpaa MI, Kukkonen H (1999) Modelling spatial contrast sensitivity functions for chromatic and luminance-modulated gratings. *Vision Res* 39:2387–2398
- Sanchez-Vives MV, Nowak LG, McCormick DA (2000) Membrane mechanisms underlying contrast adaptation in cat area 17 in vivo. *J Neurosci* 20:4267–4285
- Sceniak MP, Hawken MJ, Shapley R (2002) Contrast-dependent changes in spatial frequency tuning of macaque V1 neurons: effects of a changing receptive field size. *J Neurophysiol* 88:1363–1373
- Schmolesky MT, Wang Y, Pu M, Leventhal AG (2000) Degradation of stimulus selectivity of visual cortical cells in senescent rhesus monkeys. *Nat Neurosci* 3:384–390
- Sowden PT, Rose D, Davies IR (2002) Perceptual learning of luminance contrast detection: specific for spatial frequency and retinal location but not orientation. *Vision Res* 42:1249–1258
- Tolhurst DJ, Movshon JA, Dean AF (1983) The statistical reliability of signals in single neurons in cat and monkey visual cortex. *Vision Res* 23:775–785
- Uhlrich DJ, Essock EA, Lehmkuhle S (1981) Cross-species correspondence of spatial contrast sensitivity functions. *Behav Brain Res* 2:291–299
- Virsu V, Rovamo J (1979) Visual resolution, contrast sensitivity, and the cortical magnification factor. *Exp Brain Res* 37:475–494
- Zhou Y, Huang C, Xu P, Tao L, Qiu Z, Li X, Lu ZL (2006) Perceptual learning improves contrast sensitivity and visual acuity in adults with anisometric amblyopia. *Vision Res* 46:739–750